Iranian Journal of Oil & Gas Science and Technology, Vol. 7 (2018), No. 1, pp. 93-109
http://ijogst.put.ac.ir

A Numerical Study on Using Air Cooler Heat Exchanger for Low Grade Energy Recovery from Exhaust Flue Gas in Natural Gas Pressure Reduction Stations

Mansoor Naderi[1], Ghasem Zargar[2,*], and Ebrahim Khalili[3]

[1] M.S. Student, Department of Energy System Engineering, Petroleum University of Technology, Abadan, Iran
[2] Associate Professor, Department of Petroleum Engineering, Petroleum University of Technology, Abadan, Iran
[3] Ph.D. Candidate, National Iranian Gas Company (NIGC), Shahrekord Gas Company, Shahrekord, Iran

Received: July 16, 2016; *revised*: September 21, 2016; *accepted*: October 22, 2016

Abstract

Heat EXchangers (HEX) that are used in City Gate Station (CGS) systems are modeled numerically to recover the exhaust waste heat. It was tried to find the best viscous model to obtain results in accordance with experimental results and to change the heat exchanger design. This HEX is used for recovering heat from exhaust flue gas with a mixture of 40% water and 60% ethylene glycol as the cooling fluid. Then, the effects of sizes and numbers of fins and tube rows on recovered heat rate were investigated under various pump speeds. As the first step in solving the problem, SST k–ω and RNG k–ε suitable viscous models were chosen for these kinds of problems. Secondly, a new HEX is designed at a fixed coolant speed, pipe and fin thickness, and shell dimension because of operational constraints. Finally, the best HEX with the minimum pressure drop (minimum fin number) is numerically analyzed, and the new HEX specifications were extracted.

Keywords: Air Cooler Heat Exchanger, Gas Pressure Reduction Station, Heat Recovery Systems, Numerical Study

1. Introduction

Due to the growing energy consumption in the world, demand for extracting more energy is inevitable. Natural gas is a hydrocarbon compound which is considered as a superior energy in many countries. The distribution of natural gas resources in certain areas has led to using the transmission and distribution systems. The most economic method is pipeline transportation. Because of avoiding thick pipelines, gas compression can be used, and natural gas is transferred to gas stations at a high pressure. Gas pressure is increased from 700 to 1200 psi (Data Sheets, 2016). To deliver gas at the consumer ideal pressure, its pressure has to be reduced. Energy stored in the gas flow is released in a pressure reduction station. The outlet pressure of natural gas pressure reduction stations, depending on the city and its location, is usually 250 or 60 psi (Arabkoohsar et al., 2015). The process of gas pressure reduction occurs in throttling valves in pressure reduction stations. According to Jul-Thompson throttling process, along pressure reduction temperature is also reduced. There is little humidity in natural gas, and if its temperature is reduced lower than the specific temperature, hydrates are formed. To prevent hydrate formation in gas stations, gas must be heated before pressure

* Corresponding author:
Email: zargar@put.ac.ir

reduction. Most of the burner heat is discharged to atmosphere by flue gas as the main part of the waste heat.

It is confirmed that in heaters of a CGS system more than 50% of fuel energy is wasted from the exhaust, and just 50% of the fuel energy is converted to useful heat (Khalili et al., 2011; Data Sheets, 2016). To select an appropriate heat exchanger (HEX) design, the limitations for each HEX type should firstly be considered. Although production cost is often the primary limitation, several other selection aspects such as temperature ranges, pressure limits, thermal performance, pressure drop, fluid flow capacity, clean ability, maintenance, materials etc. are important (Edwards, 2008). These specifications (or criteria) are accepted in the designed HEX, but there is a need for optimizing old systems. One of the most effective methods to increase heat transfer is using fins, which is widely used in designing HEX. Some of the special HEX designs to recover the exhaust heat are introduced in the following. Recently, Hatami et al. in an experimental work studied that the heat recovery system of an internal combustion engine could be improved approximately by 10% at different loads and speeds of the internal combustion engine by using the recovered exergy from a simple double pipe HEX in the exhaust (Hatami et al., 2014). Moreover, Hatami et al. studied the optimal design of finned type HEX to recover waste heat from the exhaust of a diesel engine (Hatami et al., 2014). Based on the central composite design principle, fifteen HEX cases having different numbers of fins with various a height and thickness were numerically modeled using response surface methodology (RSM), and the optimization was performed to obtain the maximum heat recovery and the minimum of pressure drop along the HEX. Wang et al. (2015) evaluated flow distributions and temperature fields of a high-temperature fin-and-tube evaporator by using a CFD method and the field synergy theory; then, the simulation results were verified by an engine experiment. The results indicated that using a fin-and-tube evaporator was a feasible solution for waste heat recovery. In another experimental work, Bari and Hossain (2013) tried to use water as the working fluid to estimate the exhaust waste heat obtainable from a diesel engine using two available HEX purchased from the marketplace. After optimizing the working fluid pressure and the orientation of heat exchangers, the additional power was increased from 16 to 23.7%. Bilir et al. (2012) studied the optimization of plate fin, fin tube, and protrusion dimensions numerically using a computational fluid dynamics (CFD) program. Niamsuwan et al. (2013) designed a new economizer to achieve high heat recovery in a pasteurized milk plant. Three dimensional (3D) models including heat transfer and fluid dynamics were developed, validated by actual plant data, and used to evaluate the performance of the economizer. The simulation results indicated that the newly designed economizer could recover the heat loss of 38% and could achieve the cost saving of 13%. Pandiyarajan et al. (2011) designed a finned-tube heat exchanger, and they used a thermal energy storage using cylindrical phase change material capsules; they found out that nearly 10–15% of fuel power was stored as heat in the combined storage system at different loads. This paper aims to model the heat transfer through exhaust gases to a cold fluid using a suitable viscous model and to design a new HEX having a high performance. The numerical results are also compared with the experimental data. Also, the effects of fin number, fin size, and pump flow rate on heat recovery are graphically examined. Then, the new HEX's designed with Aspen HTFS were analyzed using CFD analysis to be compared in the same conditions.

1.1. Waste heat recovery system

In a CGS system, first, an idea of using heater waste heat for water reheating system (WR's) was presented. As shown in Figure 1, water from the bottom of heater, where the water temperature is 5 °C lower than the heater average temperature gage, is pumped to HEX by a centrifugal pump. The

water after receiving heat from the exhaust gas is drained in an expansion tank. Employing this system results in waste heat recovery.

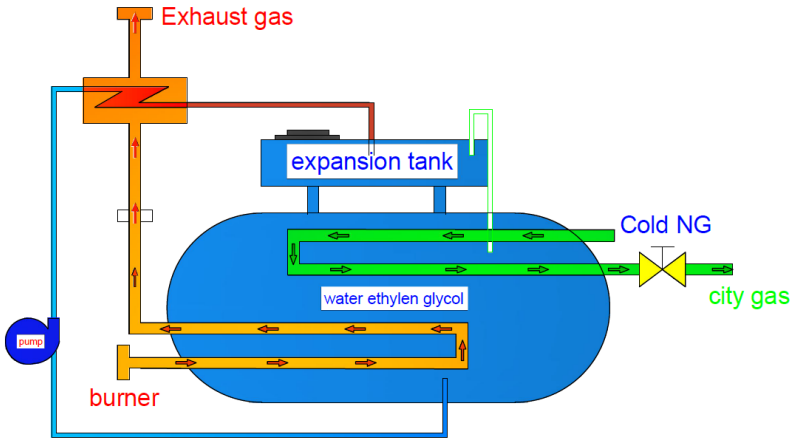

Figure 1
Schematic of water reheating system.

1.2. The case study

The case study plant is located in Shahrekord, Iran; this system is well equipped for an experimental work; an exhaust gas sampling hole is used for analyzing the exhaust gas. Temperature and mass flow rate of all the streams can be measured within a calibrated instrument, and water mass velocity is changed by a variable speed pump; fuel consumption is measured by a flow meter. Every day, month, and year the heater and city gas consumption is recorded. All the streams are insulated by fiberglass coating as displayed in Figure 2.

Figure 2
The case study system.

1.3. Assumptions

The process of the combustion in indirect heaters is assumed to be a steady state process at a constant pressure, and all the gases are assumed ideal. The density, composition, and lower heating value of natural gas are considered constant. Average air humidity ratio according to the case study condition in a combustion process is assumed 50% (Data Sheets, 2016), and the combustion reaction is considered complete.

2. Problem description

Economizers are normally designed and operated with a single pass or double passes of the exhaust gas. Heat exchangers used by researchers for exhaust waste heat recovery are selected (Figure 1). Case 1 is an air cooler HEX with a mixture of 60% water and 40% ethylene glycol circulating around the tube as the coolant and is installed in the exhaust of a CGS system. Water mass flow rates are in the range of 0.7–1.9 kg/s. Also, the temperature range for the coolant is 44 °C, and, according to natural gas consumption, it is 100–400 °C for exhaust gases in different months of year (Data Sheets, 2016). In designing the HEX, the average exhaust gas temperature is assumed 250 °C. Validation of the results needs a constant exhaust gas temperature, i.e. 350 °C. Natural gas is composed of methane, ethane, propane, and butane. The result of natural gas analysis in this case study of the CGS station is tabulated in Table 1.

Table 1
Natural gas composition.

Component	Molar percent	Minimum	Maximum
Methane (CH_4)	90.715	89.24	92.03
Ethane (C_2H_6)	3	2.41	3.77
Propane (C_3H_8)	0.64	0.25	1.03
n-butane (C_4H_{10})	0.12	0.06	0.18
i-butane (C_4H_{10})	0.13	0.02	0.24
n-pentane (C_5H_{12})	0.04	0.01	0.07
i-pentane (C_5H_{12})	0.02	0	0.04
Nitrogen (N_2)	4.415	3.73	5.1
Carbon dioxide (CO_2)	0.905	0.66	1.15
Total	100		

Therefore, the general equation of the combustion reaction of this hydrocarbon fuel with air is written as follows (Van Wylen et al., 2002):

$$\begin{aligned}&(0.907CH_4+0.0309C_2H_6+0.0064C_3H_8+0.0025C_4H_{10}+0.006C_5H_{12}+0.0441N_2+0.00905CO_2)\\&+(1.975+\lambda)\times(O_2+3.76N_2+4.76\times1.61\omega H_2O)\rightarrow \alpha CO_2+\beta H_2O+\delta O_2+\gamma N_2\end{aligned} \quad (1)$$

where, λ parameter represents the equivalence ratio and shows the percentage of excess air. ω parameter is the humidity ratio of the environment. Regarding the molar balance in the combustion equation, excess air and exhaust gases mass flow rates are respectively equal to 81% and 0.0525 kg/s. Table 2 shows the combustion product components (Data Sheets, 2016).

Table 2
Flue gas component.

Component	O_2	CO_2	H_2O	N_2
Fraction (%)	10.85	6	10.15	73

This work focuses on modifying the pattern piping coil and the number of fins to achieve the minimum pressure drop in the shell side and to prevent flame off with a minimum pump head. Thus, it is needed to model the HEX numerically using a commercial CFD code in FLUENT. The meshing

was generated in GAMBIT and exported to FLUENT after defining boundary conditions (Canonsburg, 2013).

3. Geometry summery

Air cooler HEX specification is listed in Table 3.

Table 3
Heat exchanger specification.

Dimensions	
Tube thickness (mm)	1.2
Tube outside diameter (mm)	97
Tube length in pass (mm)	70
Fin surface (m^2)	0.056
Fin thickness (mm)	0.15
Number of fin per inch	7
Number of passes	2
Number of tube in passes	4
Number of tube rows	24
Exhaust gas pipe diameter (mm)	60

Figures 3-5 show the schematic of header, fin, and stream respectively, and Figure 6 displays the case study geometry of the HEX. The geometric model of the HEX is very complicated, so it needs a long time to be simulated in each run. By the assumption of a uniform stream in the cold and hot sides of the HEX, as shown in Figure 6, one pass of the HEX was selected for modeling (Sanaye and Dehghandokht, 2011; Niamsuwan et al., 2013). The detailed design of the economizer is illustrated in Figures3-6; it consists of a rectangular shell, and the bundle of the tubes is fixed in the middle of the shell. There are four rows of tubes (with two passes) in the gas flow direction with twenty four tubes in every row. Finally, the outlet water at a high temperature is delivered from the top header to the expansion tank of the heater.

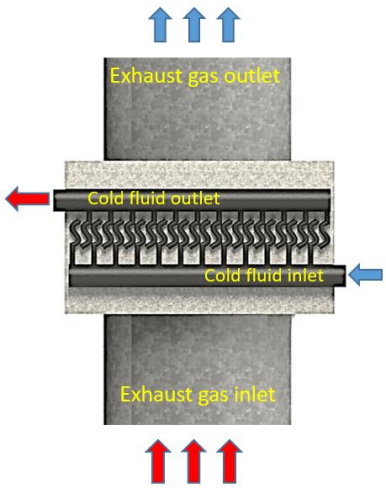

Figure 3
Schematic of flow and header.

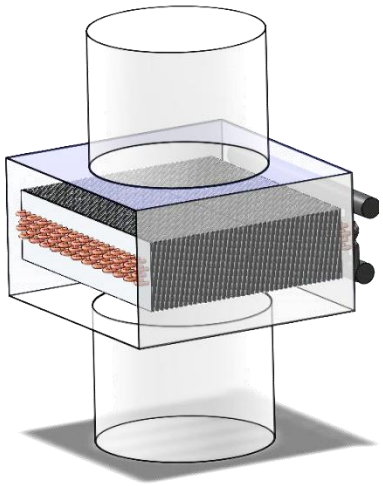

Figure 4
Schematic of baffle and pipe in the shell.

Figure 5
Schematic of baffle and pipe orientation.

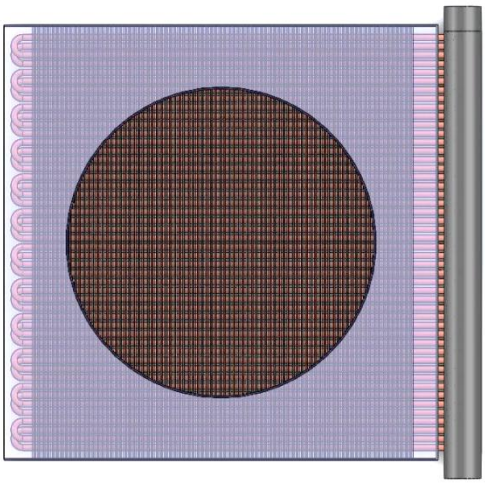

Figure 6
Schematic of baffle and pipe by top view.

4. Governing equations

A model is described on account of the structure of the designed HEX shown in Figure 5. A mathematical model is developed based on three dimensional heat transfer by including the fluid dynamic on the both fluid sides. The governing equations consist of general heat transfer equation continuity, energy and Navier-Stokes momentum equations (Fox et al., 2004; Rehman, 2011), and SST k–ω and RNG k–ε (Nikou and Ehsani, 2008; Hatami and Ganji, 2014).

Continuity equation:

$$\nabla \times (\rho \vec{V}) = 0 \tag{2}$$

Momentum equations:

x-momentum:

$$\nabla \times (\rho u \vec{V}) = -\frac{\partial p}{\partial x} + \frac{\partial \tau_{xx}}{\partial x} + \frac{\partial \tau_{yx}}{\partial y} + \frac{\partial \tau_{zx}}{\partial z} \tag{3}$$

y-momentum:

$$\nabla \times (\rho v \vec{V}) = -\frac{\partial p}{\partial y} + \frac{\partial \tau_{xy}}{\partial x} + \frac{\partial \tau_{yy}}{\partial y} + \frac{\partial \tau_{zy}}{\partial y} \tag{4}$$

z-momentum:

$$\nabla \times (\rho w \vec{V}) = -\frac{\partial p}{\partial z} + \frac{\partial \tau_{xz}}{\partial x} + \frac{\partial \tau_{yz}}{\partial y} + \frac{\partial \tau_{zz}}{\partial z} \tag{5}$$

Energy equation:

$$\rho c_p \left(u \frac{\partial T}{\partial x} + v \frac{\partial T}{\partial y} + w \frac{\partial T}{\partial z} \right) = \lambda \left(\frac{\partial^2 T}{\partial x^2} + \frac{\partial^2 T}{\partial y^2} + \frac{\partial^2 T}{\partial z^2} \right) \tag{6}$$

In this paper, two viscous models are examined. ReNormalization-Group (RNG) k–ε model (standard) and Shear-Stress Transport (SST) k–ω. These two models were selected because previous studies, which are reviewed elsewhere (Nikou and Ehsani, 2008; Hatami and Ganji, 2014), introduced these models as efficient models. For RNG k–ε model, thermal effect is considered in the enhanced wall treatment panel. Transport equations for RNG k–ε model in a general form are given by (Hatami and Ganji, 2014):

$$\frac{\partial}{\partial t}(\rho\varepsilon) + \frac{\partial}{\partial x_i}(\rho\varepsilon u_i) = \frac{\partial}{\partial x_j}\left(\alpha_\varepsilon \mu_{eff} \frac{\partial \varepsilon}{\partial x_j} \right) + C_{1\varepsilon} \frac{\varepsilon}{k}(G_k + G_{3\varepsilon} G_b) - C_{2\varepsilon} \rho \frac{\varepsilon^2}{k} - R_\varepsilon - S_\varepsilon \tag{7}$$

$$\frac{\partial}{\partial t}(\rho k) + \frac{\partial}{\partial x_i}(\rho k u_i) = \frac{\partial}{\partial x_j}\left(\alpha_k \mu_{eff} \frac{\partial k}{\partial x_j} \right) + G_k + G_b - \rho\varepsilon - Y_M + S_k \tag{8}$$

where, G_k represents the generation of turbulence kinetic energy due to the mean velocity gradients and G_b is the generation of turbulence kinetic energy due to buoyancy; $C_{1\varepsilon}$= 1.42 and $C_{2\varepsilon}$= 1.68 in RNG k–ε model (Hatami and Ganji, 2014). Transport equations for SST k–ω are defined by (Hatami and Ganji, 2014):

$$\frac{\partial}{\partial t}(\rho k) + \frac{\partial}{\partial x_i}(\rho k u_i) = \frac{\partial}{\partial x_j}\left(\Gamma_k \frac{\partial k}{\partial x_j} \right) + G_k - Y_K + S_K \tag{9}$$

$$\frac{\partial}{\partial t}(\rho\omega) + \frac{\partial}{\partial x_i}(\rho\omega u_i) = \frac{\partial}{\partial x_j}\left(\Gamma_\omega \frac{\partial \omega}{\partial x_j} \right) + G_\omega - Y_\omega + S_\omega \tag{10}$$

As an approximation, the properties of natural exhaust gas are calculated by Aspen Properties software, and the changes in some temperature-dependent properties due to a low temperature in exhaust are ignored. The variations in the properties of the exhaust gases are shown in Figure 7. For each property, a fourth order polynomial is plotted, the equation and coefficients of which are calculated using the mixing law and Perry's handbook correlations for the properties of individual species (Table 4) (Golshadi et al., 2013; Tilton and Hottel, 2008). The solid phases, i.e. tubes and fins, are considered to be carbon steel, the thermal properties and the cold fluid properties of which are tabulated in Table 5. A mixture of 40% water and 60% ethylene glycol is considered for the coolant fluid.

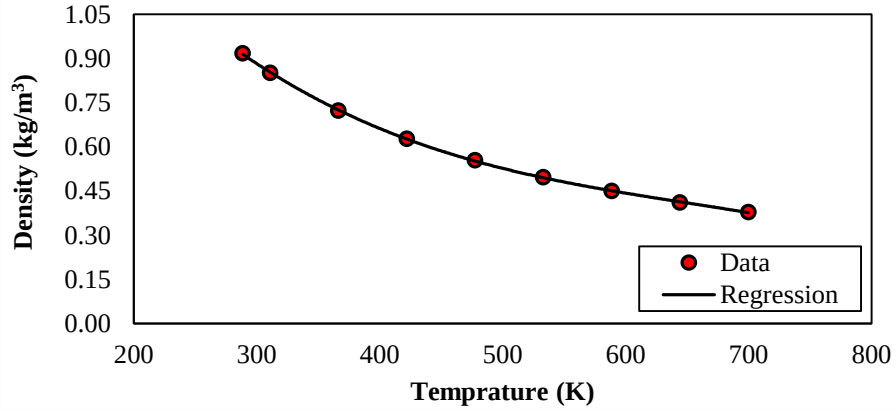

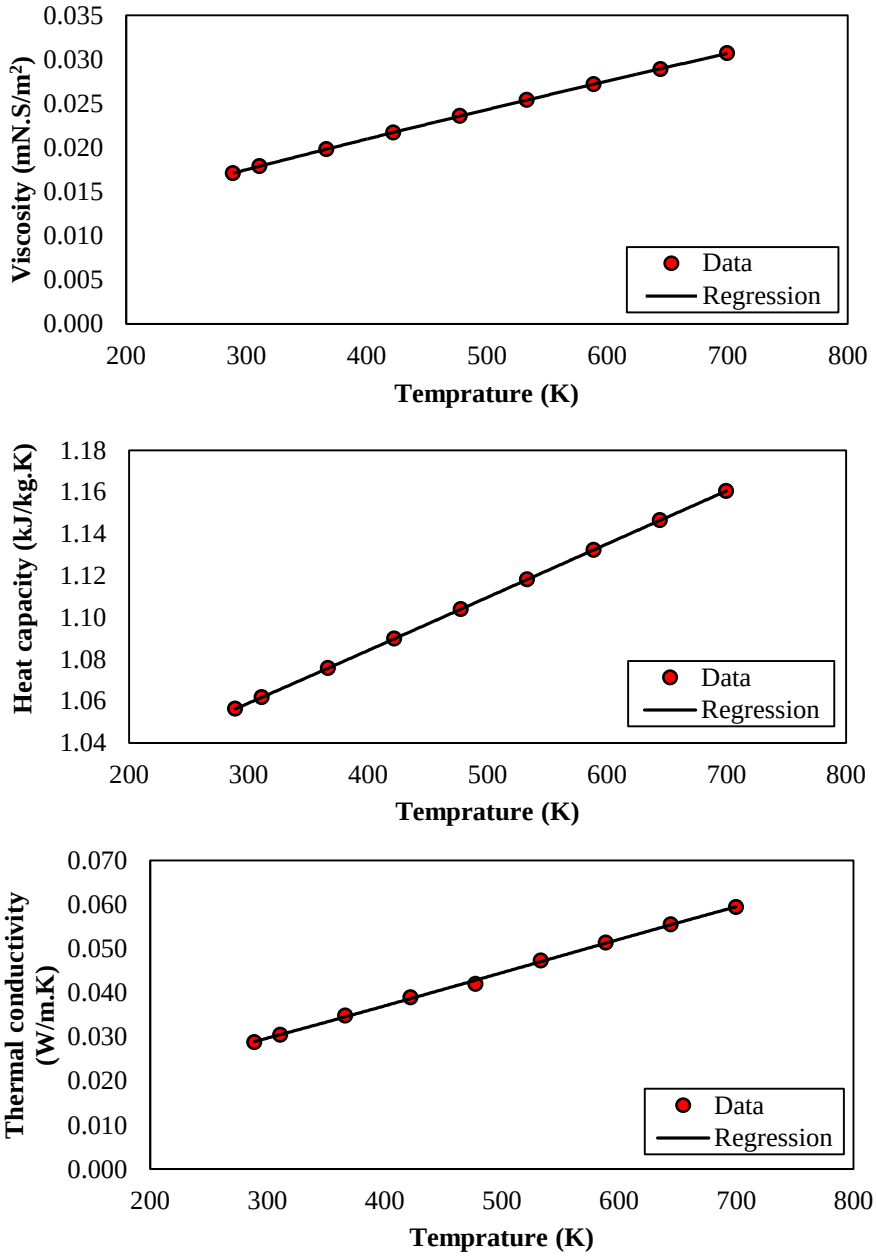

Figure 7
Temperature-dependent properties of the exhaust gas.

Table 4
The coefficients of the polynomial functions correlating the exhaust gas properties.

Exhaust gas property	$f(t) = At^3 + Bt^2 + Ct + D$			
	A	***B***	***C***	***D***
Density (kg/m^3)	-3.963×10^{-9}	5.342×10^{-6}	-0.00293	0.9557
Viscosity (N.s/m^2)	-6.600×10^{-16}	-5.016×10^{-12}	3.536×10^{-8}	1.656×10^{-5}
Heat capacity (kJ/kg.K)	-3.198×10^{-11}	2.454×10^{-8}	2.488×10^{-4}	1.052
Thermal conductivity (W/m.K)	2.109×10^{-13}	-7.598×10^{-9}	7.787×10^{-5}	0.02758

Table 5
Thermal properties of the coolants and the solid phases.

Material	Density (kg/m^3)	Viscosity ($N.s/m^2$)	*Cp* (kJ/kg.K)	*K* (W/m.K)
Water	992.69	0.598×10^{-6}	4.187	0.626
Ethylene glycol	1093.23	8.537×10^{-6}	2.465	0.267
Water–ethylene glycol (40%/60%)	1050.66	1.339×10^{-6}	3.154	0.411
Aluminum (fin) (*t*= 400)	2702.00	-	903.000	240.000
Copper (pipe) (*t*= 400)	8933.00	-	385.000	393.000

At first, for case one, a model with six mesh numbers using water-ethylene glycol as the coolant is constructed to show the mesh independency. Figure 8 shows element meshes representing the structural mesh. The error in the prediction of temperature at a coolant flow rate of 1.9 kg/s and at a mesh density of 800,000 is 4%; however, a mesh density of 600,000 leads to an error of 8% in the predication of temperature in similar conditions; on the other hand, the simulation runtime at a mesh density of 800,000 is approximately 50% greater than that at a mesh density of 600,000. Thus, in this work, by considering both the computational time and the accuracy of the results, a mesh density of 6000,000 was selected (Hosseini et al., 2015).s

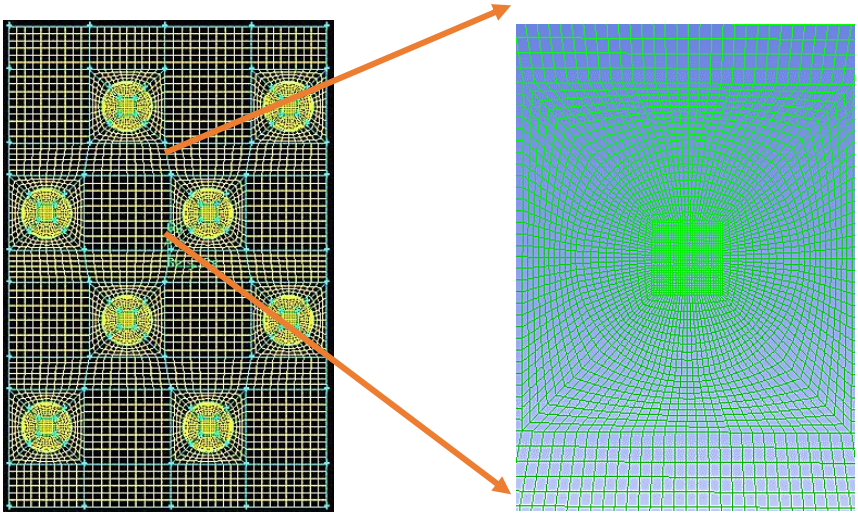

Figure 8
Model converged mesh.

Figure 9 shows the average temperature of the exhaust gas at different mesh densities and at a coolant flow rate of 1.9 kg/s. The criterion and method for mesh independency are similar to the study carried out by Hosseini et al. (2015).

5. Validation

To evaluate the performance of the heat exchanger designed based on the mathematical model, it was essentially validated by the observed data. The dynamic temperature profiles for both water and exhaust gas were gathered by the observation in the real CGS system, where the HEX was implemented into the CGS system. Water temperature profiles at the inlet and outlet of the newly designed economizer were recorded by a temperature gauge installed on the piping system (Figure10). The temperature profiles of the exhaust gas were measured using a digital thermocouple recording

data before and after the HEX. The data were also measured at various pump speeds. The outlet exhaust gas and coolant temperatures were compared to the simulation data, and the exhaust gas and water temperature profiles were validated with the model results (Sabziani and Sari, 2015). The location where the thermocouples are installed in the experimental conditions results in difference between the outlet temperatures of the experimental setup and that of the numerical modeling since the thermocouples measure the temperature at a point, while the numerical modeling calculates the average surface temperature (Niamsuwan et al., 2013).

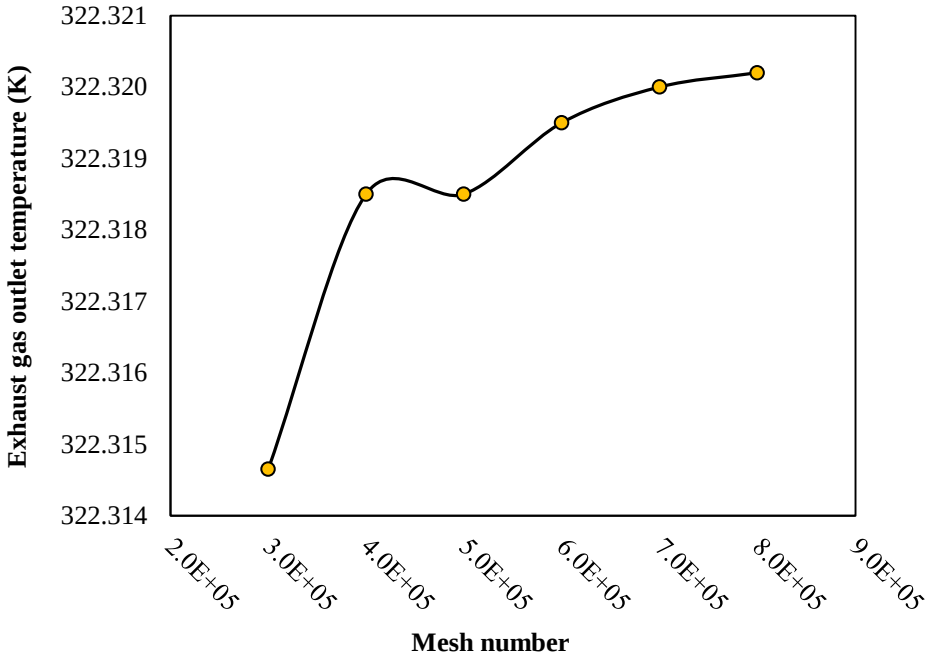

Figure 9
Exhaust gas outlet temperature.

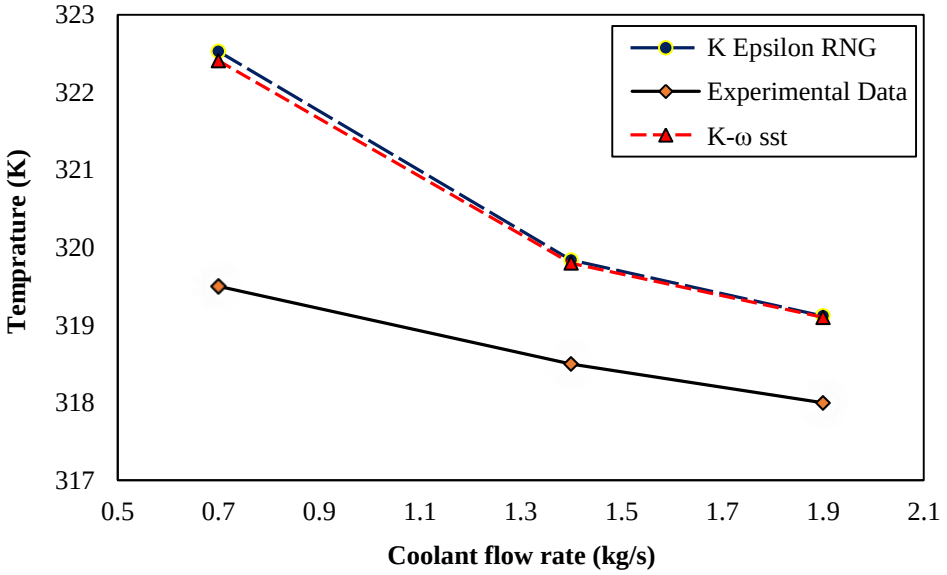

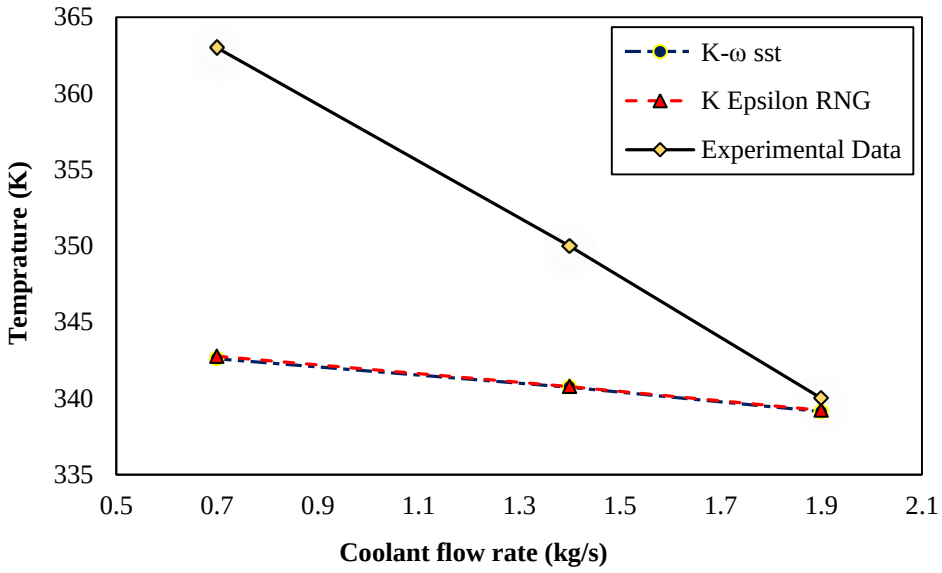

Figure 10
Comparison of three viscous models with the experimental outcomes at different coolant flow rates.

As mentioned before, the case studies shown in Figure 2 were modeled numerically at different pump speeds; furthermore, four different geometries were considered for case 2 to show the effect of fin number and pipe arrays. The modeling accuracy was compared to the experimental outcomes. These figures confirm that SST k–ω is a suitable viscous model for these problems since its results are closer to the experimental data; but, its convergence is more difficult compared to RNG k–ε. The contours of the temperatures at three coolant flow rates (0.7, 1.4, and 1.9 kg/s) and at an exhaust gas temperature of 350 °C are displayed in Figure 11. It is obvious that by increasing the coolant flow rate, the exhaust gas outlet temperature is decreased.

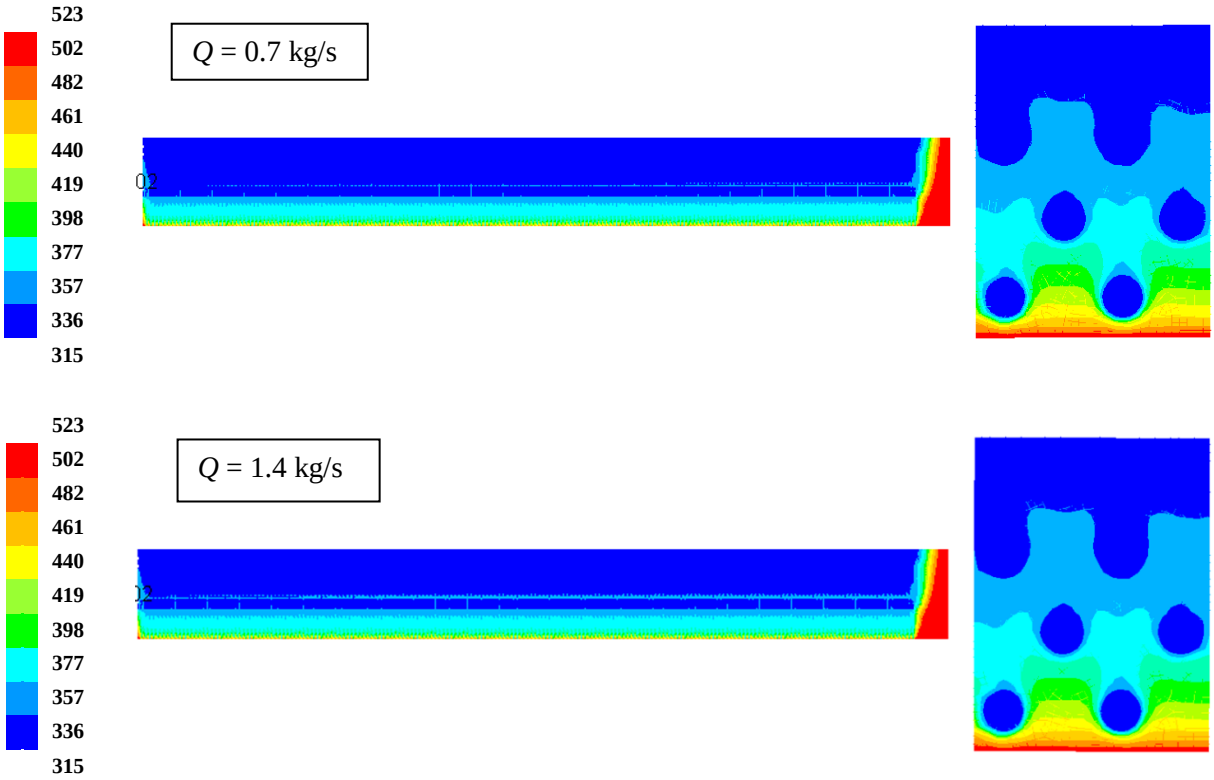

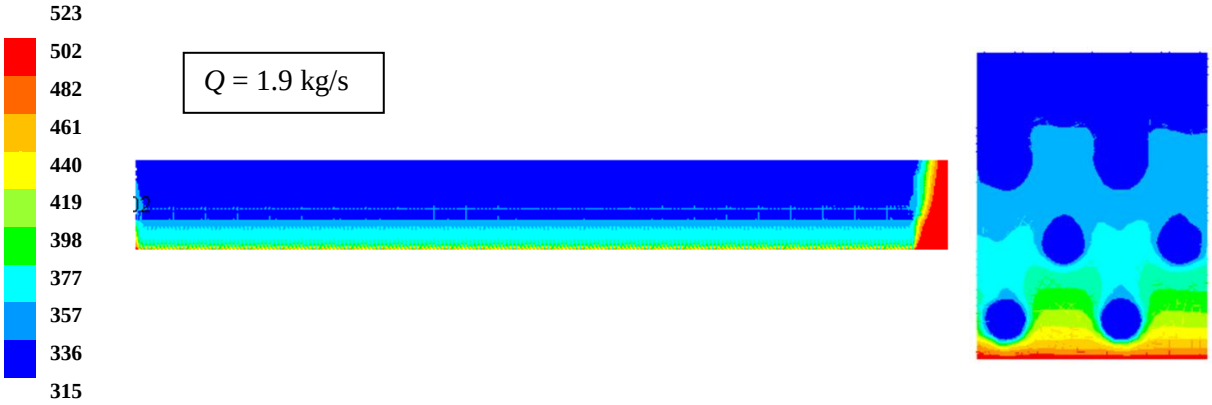

Figure 11
Temperature counters in the shell side.

6. Results and discussion

The results of the case study modeling show that this HEX works with an inefficient heat transfer coefficient and a high pressure drop in the exhaust gas side, which causes burner to flame off. Therefore, it is needed to change the design of the HEX. The new designed HEX has some criteria such as the minimum coolant mass velocity and pressure drop in the flue gas side. By fixing tube and fin thickness and lowering the shell dimensions, the new HEX was designed using Aspen HTFS software. In all the cases with similar tube rows (at different tube angles of 30, 45, 60, and 90°), the tubes with an angle of 30° have the minimum fin material and a lower pressure drop in the shell side compared to the first models. The new designed HEX's are shown in Tables 6-8.

Table 6
Heat exchanger designed with four-tube rows.

No. HEX	Coolant flow (kg/s)	Fin per inch	No. circuit	HEX. total weight (kg)	Transverse pitch (cm)	Coolant outlet temperature (°C)	Pipe pressure drop (kPa)
1	1	3.5	6	12.07	3.8	47	3.51
2	1.2	3.4	7	14.07	3.6	46.5	3.69
3	1.3	3.3	8	16.06	3.4	46.3	3.35
4	1.5	3.4	9	18.07	3.2	46	3.50
5	1.65	3.5	10	20.07	2.8	45.8	3.42
6	1.82	3.6	11	22.08	2.6	45.7	3.43
7	1.95	3.7	12	24.08	2.4	45.5	3.31
8	2.12	3.9	13	26.09	2.2	45.4	3.25

Table 7
Heat exchanger designed with five-tube rows.

No. HEX	Coolant flow (kg/s)	Fin per inch	No. circuit	HEX. total weight (kg)	Transverse pitch (cm)	Coolant outlet temperature (°C)	Pipe pressure drop (kPa)
1	1	3.5	6	12.1	3.8	47.0	3.5
2	1.2	3.4	7	14.1	3.6	46.5	3.7
3	1.3	3.3	8	16.1	3.4	46.3	3.3
4	1.5	3.4	9	18.1	3.2	46.0	3.5
5	1.65	3.5	10	20.1	2.8	45.8	3.4
6	1.82	3.6	11	22.1	2.6	45.7	3.4
7	1.95	3.7	12	24.1	2.4	45.5	3.3
8	2.12	3.9	13	26.1	2.2	45.4	3.2

Table 8
Heat exchanger designed with six-tube rows.

No. HEX	Coolant flow (kg/s)	Fin per inch	No. circuit	HEX. total weight (kg)	Transverse pitch (cm)	Coolant outlet temperature (°C)	Pipe pressure drop (kPa)
1	1.2	2.7	6	14.5	3.8	46.3	3.533
2	1.4	2.7	7	16.9	3.6	46.1	3.764
3	1.6	2.6	8	19.3	3.4	45.9	3.53
4	1.8	2.7	9	21.7	3.2	45.6	3.526
5	1.95	2.8	10	24.4	2.8	45.5	3.353
6	2.2	2.8	11	26.5	2.6	45.4	3.33
7	2.4	2.9	12	28.9	2.4	45.3	3.481
8	2.6	3	13	31.3	2.2	45.2	3.46

All the samples were designed for satisfying the minimum coolant velocity in tube and the maximum heat recovery at different pump speeds. Figure 12 shows fin number change in different tube rows.

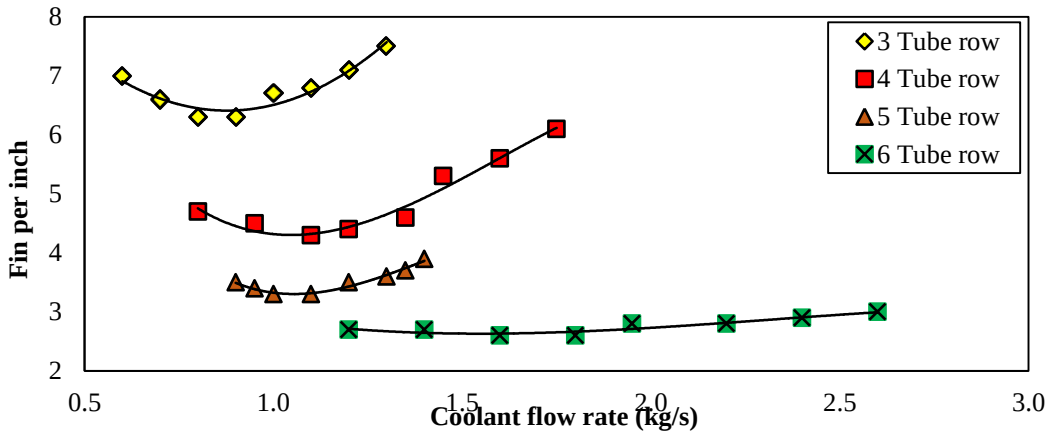

Figure 12
Changing fin number at different coolant flow rates and using various pipe arrays.

The samples having the minimum fin per inch, and thus causing the minimum pressure drop, are highlighted in each table (Tables 6-8) (Falavand and Ghafouri, 2015). The number of generated meshes for the selected sample is similar to a case study system used. The converged mesh number of the selected heat exchanger is listed in Table 9.

Table 9
Converged mesh number of the selected heat exchanger.

Number of tube rows	Converged mesh number
4	560000
5	600000
6	620000

The temperature contours plotted for designing the HEX at 250 °C are shown in Figure 13. Because of equaling tube length with the exhaust gas pipe diameter and using a uniformed flow distribution, this model is more accurate than the previous one.

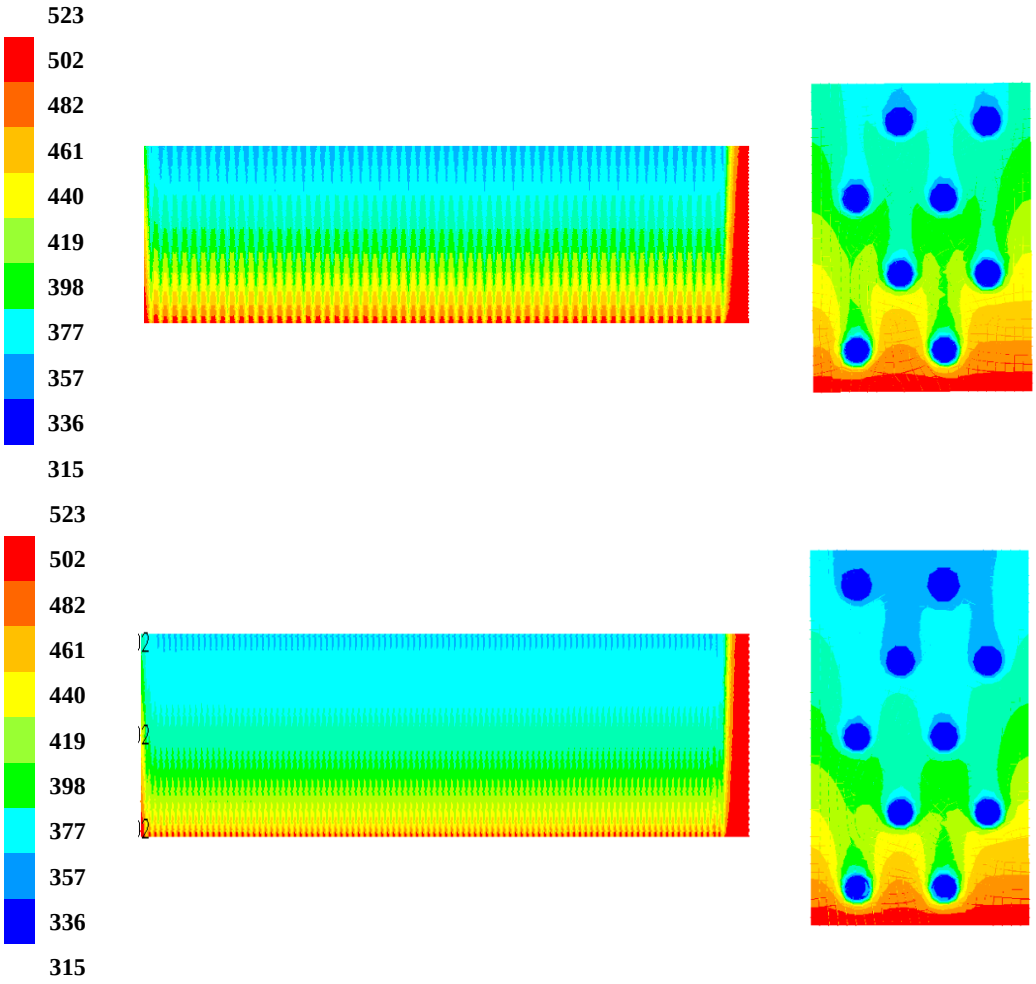

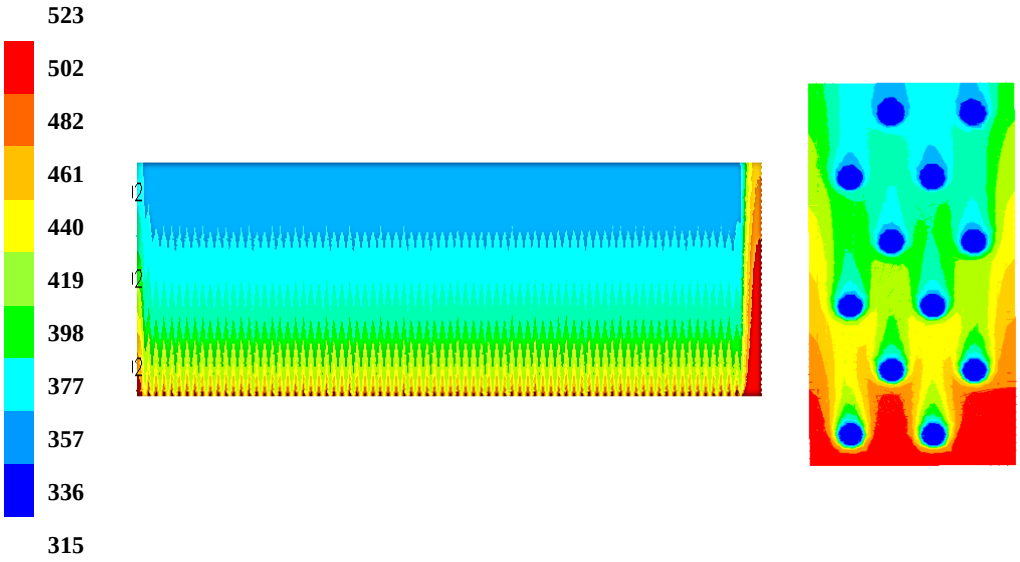

Figure 13
Proposed HEX temperature counters.

The results of the numerical study shows that the pressure drop in the exhaust gas side in case 2 is the minimum among all the designed HEX's, and case 1 has a higher pressure drop in comparison to the first model; also, case 3 has the minimum coolant pressure among the cases. In general, case 2 was selected for the case study, and all the heaters had a capacity of around 20000 SCMH in the CGS system.

7. Conclusions

Waste energy recovered by using air cooler HEX in gas pressure reduction station systems was studied numerically. The heat transfer through the walls and fins was successfully modeled, and the heat transferred to the cooling fluid was calculated as the recovered heat. The results show that SST k–ω and RNG k–ε are suitable viscous models. Moreover, graphs and contours reveal that the recovered heat can be improved by decreasing the shell dimensions, and consequently the pressure drop in the shell side is minimized. The temperatures of the outlet exhaust gas and water confirm that RNG k–ε and SST k–ω calculate the outlet cold fluid temperatures of all the samples close to the experimental results at different pump speeds. The new designed HEX was used for optimizing this economizer in the CGS system. The new HEX's were numerically studied, and the one with the minimum pressure drop in the exhaust gas side was selected as the ideal HEX. The result of this study can be expanded for all the CGS systems having a capacity of about 20000 SCMH. Studying the feasibility of using this waste heat recovery (WHR) system in a CGS system at different heater capacities from energy, exergy, economic, and thermoseconomic points of view is recommended for future work. Plate fin heat exchanger can also be optimized by using genetic algorithm.

Acknowledgements

The authors gratefully acknowledge Shahrekord Gas Company employees for helping us with providing the experimental equipment and obtaining the results and for their constructive suggestions.

Nomenclature

CFD	: Computational fluid dynamics
CGS	: City gate station

HEX	: Heat exchanger
LHV	: Lower heating value
RNG	: Renormalization group
RSM	: Response surface methodology
SCMH	: Standard cubic meter per hour
SST	: Shear stress transport
WHR	: Waste heat recovery
WRs	: Water reheating system
λ	: Excess air
ω	: Humidity ratio

References

Arabkoohsar, A., Farzaneh-gord, M., Deymi-dashtebayaz, M., Machado, L., and Koury, R.N.N., A New Design for Natural Gas Pressure Reduction Points by Employing a Turbo Expander and a Solar Heating Set, Renewable Energy, Vol. 81, p. 239–250, 2015.

Bari, S. and Shekh N. H., Waste Heat Recovery from a Diesel Engine Using Shell and Tube Heat Exchanger, Applied Thermal Engineering, Vol. 61, No. 2, p. 355–363, 2013.

Bilir, L., Ilken, Z., and Erek, A., Numerical Optimization of a Fin-tube Gas to Liquid Heat Exchanger, International Journal of Thermal Sciences, Vol. 52, p. 59-72, 2012.

Canonsburg Technology Drive, ANSYS Fluent Tutorial Guide, 15317 (November): p. 724–746, 2013.

Data Sheets, taken from Shahrekord Gas Pressure Reduction Station, Iran, 2016.

Edwards, J. E., Design and Rating Shell and Tube Heat Exchangers, Teesside, Ukraine, 2008.

Falavand, J.A. and Ghafouri, A., Optimization of Fin Type and Fin per Inch on Heat Transfer and Pressure Drop of an Air Cooler, Optimization, Vol. 9, No. 9, p. 1607–1610, 2015.

Fox R.W., Mcdoland, M.T., and Prichard, P.J., Introduction to Fluid Mechanics," John Wiley & Sons, New York, 2004.

Golshadi, M., Mosayebi Behbahani, R., and Irani, M.R., CFD Simulation of Dimethyl Ether Synthesis from Methanol in an Adiabatic Fixed-bed Reactor, Iranian Journal of Oil & Gas Science and Technology, Vol. 2, No. 2, p. 50–64, 2013.

Hatami, M. and Ganji, D.D., Case Studies in Thermal Engineering Numerical Study of Finned type Heat Exchangers for ICE's Exhaust Waste Heat Recovery, Case Studies in Thermal Engineering, Vol. 4, p. 53–64, 2014.

Hatami, M., Jafaryar, M., Ganji, D.D., and Gorji-bandpy, M., Optimization of Fined-tube Heat Exchangers for Diesel Exhaust Waste Heat Recovery Using CFD and CCD Techniques, International Communications in Heat and Mass Transfer, Vol. 57, p. 254–263, 2014.

Hosseini, S.M., Shahbazi, K., and Khosravi Nikou, M.R., A CFD Simulation of the Parameters Affecting the Performance of Downhole De-oiling Hydrocyclone, Iranian Journal of Oil & Gas Science and Technology, Vol. 4, No. 3, p. 77–93, 2015.

Khalili, E., Hoseinalipour, M., and Heybatian, E., Efficiency and Heat Losses of Indirect Water Bath Heater Installed in Natural Gas Pressure Reduction Station: Evaluating a Case Study in Iran, in proceedings of 8th National Energy Congress, Shahrekord, Iran, 2011.

Niamsuwan, S., Kittisupakorn, P., and Mujtaba, I.M., A Newly Designed Economizer to Improve Waste Heat Recovery: a Case Study in a Pasteurized Milk Plant, Applied Thermal Engineering, Vol. 60, No. 1–2, p. 188–199, 2013.

Nikou, M.K. and Ehsani, M.R., Turbulence Models Application on CFD Simulation of Hydrodynamics, Heat and Mass Transfer in a Structured Packing, International Communications in Heat and Mass Transfer, Vol. 35, No. 9, p. 1211-1219, 2008.

Pandiyarajan, V., Chinna Pandian, M., Malan, E., Velraj, R., and Seeniraj, R. V., Experimental Investigation on Heat Recovery from Diesel Engine Exhaust Using Finned Shell and Tube Heat Exchanger and Thermal Storage System, Applied Energy, Vol. 88, No. 1, p. 77–87, 2011.

Rehman, U., Heat Transfer Optimization of Shell and Tube Heat Exchanger through CFD Studies, Master Thesis, Calmers University of Technology, Sweden, 2011.

Sabziani, J. and Sari, A., A CFD Simulation of Hydrogen Production in Microreactors, Iranian Journal of Oil & Gas Science and Technology, Vol. 4, No. 1, p. 35–48, 2015.

Sanaye, S. and Dehghandokht, M., Modeling and Multi-objective Optimization of Parallel Flow Condenser Using Evolutionary Algorithm, Applied Energy, Vol. 88, No. 5, p. 1568–1577, 2011.

Tilton, J. N. and Hottel, H. C., Perry's Chemical Engineering's Handbook 8th Ed., McGraw-Hill Publication, 2008.

Van Wylen, G. J., Sonntag, R. E., and Borgnakke, C., Fundamentals of Thermodynamics, John Wiley and Sons, New York, 2002.

Wang, E., Zhang, H., Fan, B., Ouyang, M., Yang, K, Yang, F., Li, X., and Wang, Z., 3D Numerical Analysis of Exhaust Flow inside a Fin-and-tube Evaporator Used in Engine Waste Heat Recovery, Energy, Vol. 82, p. 800–812, 2015.